Numerical Analyses of Heat Transfer and Fluid Flow in a Corrugated Duct

Hashem Shatnawi and Abdulrahman Aldossary

Jubail Technical Institute, Jubail, Saudi Arabia
Hashem121@yahoo.com

Received: 31/08/2020
Accepted:15/11/2020

ABSTRACT- Steady laminar two-dimensional and forced convection in a corrugated duct with different configurations and flow conditions were investigated numerically. The full Naiver-Stokes and energy equation were considered. These equations have been solved using the finite element method. Flow-fields were obtained for various flow conditions. The flow patterns and reattachment indicate a firm agreement with those in the literature. It has been noticed that the maximum value of the local Nusselt number occurs near the reattachment point. The 45-to-50-degree corrugation angle provides the heights Nusselt number by 1 to 2 percent and the lowest pressure drop compared to larger or smaller angles. The influence of the Prandtl number on the thermal performance was considered, as the Prandtl number increases the average Nusselt number grows. The enhancing performance of heat transfer rate is more effective for P_r >1.

Keywords*: Corrugated channel, Heat Transfer Enhancement, Nusselt Number, Pressure drop, Solar collectors.*

المستخلص – تم دراسة الجريان المستقر و الحمل الحراري القسري عددياً في قناة متعرجة ثنائية الأبعاد ذات ابعاد وظروف تدفق مختلفة وذلك باستخدام معادلات الحركة الكاملة ومعادلة حفظ الطاقة . وقد تم حل هذه المعادلات بتحويلها من معادلات مشتقة جزئيا الى مجموعة معادلات جبرية. تم الحصول على ظروف التدفق من خلال تطبيق شروط تدفق مختلفة. لوحظ وجود توافق مع الدراسات السابقة من حيث طريقة جريان المائع ونقطة التقاء المائع مع الجدار. ولقد لوحظ ايضا أن القيمة القصوى لرقم نوسلت الموضعية تحدث بالقرب من نقطة التقاء المائع مع الجدار. وايضا ان زاوية التعرج في المجال(45 إلى 50 درجة) تعمل على زيادة رقم نوسلت بنسبة من 1 إلى 2 في المئة كما انها توفر أقل انخفاض في الضغط مقارنة مع الزوايا الأكبر و الأصغر.كما تم دراسة تأثير رقم براندل على الأداء الحراري للقناة، بزيادة رقم براندل يزداد رقم نوسلت وبالتالي يتحسن انتقال الحرارة ، وكلما كان رقم براندل اكبر كان انتقال الحرارة أفضل.

INTRODUCTION

There are several different cross-sectional duct shapes that have a potential in heat transfer. The need for more effective heat-exchanger devices resulted in the creation of a range of unconventional internal flow channels. The compact heat exchangers, solar collectors, or PV cells required different cooling techniques to reduce the operating temperature.

Corrugated ducts have been employed in several engineering devices because their efficient heat transfer capability decreases the physical size of the heat exchanger. Their efficiency is improved by the corrugations form a large surface area by volume unit, which increases the area of heat transfer. In particular, corrugated heat exchangers have been widely adopted for systems that need high thermal efficiencies, such as aerospace and gas turbine power plants [1].

Several studies have been made of corrugated ducts O'Brien et al. [2] analyzed heat transfer and pressure drop inside a corrugated duct, with 30 degrees as corrugation angle, the interval distance equal to the corrugation angle, and a rise in the heat transfer was correlated with the corrugation duct.

P. J. Oliveira [3] studied Newtonian laminar flow and pressure drop coefficient for sudden axisymmetric expansions numerically, and he concluded that the local loss factor was expected to abruptly increase in 1:26 for Reynolds inlet between 1 and 225. The numerical analysis and efficiency modeling of a rapid fence expansion has been conducted by D. K. Mandal et al. [4], the estimation of the lower Reynolds number regime

indicates that the productivity of the fence benefits depending on the location of the fence and the relaxed angle of the fence.

Jia Jun Lim et al. [5] numerically analyzed of sudden expansion structure supercritical flow. The high-speed flow from the expansion flows through the channel and mirrored on the sidewall, and this mechanism contributes to a rise in the hill-shaped region of the sidewall depth.P. Rajesh Kanna et al. [6] studied the Conjugate heat transfer numerically from sudden expansion using nanofluid, local Nusselt number Attains high values close to the contact point and approaches the downstream asymptotic value. The eddy and volume fraction of the bottom wall show a major effect on the average number of Nusselt.

Khudheyer S. et al. [7] investigated the laminar flow numerically in a sudden expansion obstacles channel. The findings show that obstacles have a significant impact on flow dynamics and heat transfer development. Moreover, heat transfer is improved by increasing the thickness of obstacles and this phenomenon is diminished by increasing the length of the obstacles. Gerardo N. et al. [8] investigated two-dimensional steady-state viscoelastic flows through asymmetric expansion, for the Newtonian case, a dissimilarity of asymmetrical flow for Reynolds numbers above 36 was observed.

Li-Zhi Zhang[9] studied numerically 3-dimensional heat transfer and fluid flow of air in a cross-corrugated triangular channel. The corrugated ducts were found to increase heat transfer by 40 to 60 % but with a double pressure decrease penalty. N. El-Menshawy has experimentally explored fluid flow and heat transfer over a rectangular repeated corrugated duct, and he found that the location of reattachment depends on corrugation angles.

A corrugated duct can be used on a solar collector or solar Panel cooling system. M.N Metwally et al. investigated the performance analysis experimentally on a corrugated duct solar collector as an air heater; the efficiency of the collector increased by 15-43% [10]. K. A. Shockey et al. [11] experimentally studied the heat transfer for solar air collectors with a Back-corrugated absorber; two corrugated-plate configurations created two different heat transfer characteristics on the upper and lower plate and the corrugated absorber's heat transfer efficiency is much better than the standard flat absorber. A. Álvarez et al. [12] examined experimentally and numerically a corrugated solar thermal collector, the improved performance obtained for the corrugated collector is equal to 86%.

The objective of this work is to investigate the effect of the corrugation of a 2-D channel on the fluid characteristics and heat transfer performance. Study also the impact of the number of Reynolds number, step height, corrugation angle, and Prandtl number on the heat transfer and separation, in addition to that finding the effective corrugation angle in which the heat transfer performance is the maximum and the pressure drop is the minimum.

MATHEMATICAL MODEL

Numerical solutions of the conservation equation investigated for the physical corrugated, open channel as depicted schematically in figure 1. The geometry of the channel is detailed by the corrugation angle α [degree], the step height H [m], the vertical distance between the wall before the corrugation H_1[m], the axial length of the lower heated wall L[m]. The flow enters the hydrodynamic entrance L_e [m] with a uniform velocity u_{in} [m/sec] and with inlet temperature T_{in} [K]. Laminar flow was measured with Reynolds number range 50-500; the reason beyond selecting this range is to capture the flow transition from symmetry flow to un-symmetry.

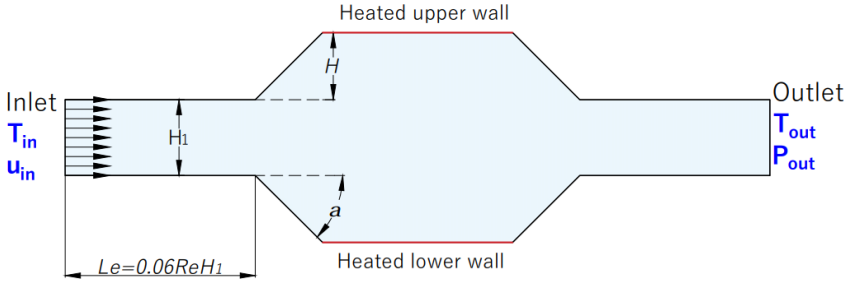

Figure 1: A schematic model of a corrugated duct with boundary condition

The velocity profile becomes fully developed. The boundary conditions at the upper and lower wall are constant temperature T_w [K], where $T_w > T_{in}$. The dimensionless step height *He*=H/H1. The pressure (P_{out})at the outlet of the computational domain is taken equal to zero gauges.

Governing Equations

For incompressible steady-state laminar flow, with constant Thermos-physical characteristics, the governing equation can be expressed in dimensionless form as follow [13]:

$$\frac{\partial u}{\partial x} + \frac{\partial v}{\partial y} = 0 \quad (1)$$

The momentum equations are:

$$u\frac{\partial u}{\partial x} + v\frac{\partial u}{\partial y} = -\frac{\partial p}{\partial x} + \frac{1}{\mathbf{Re}}\left(\frac{\partial^2 u}{\partial x^2} + \frac{\partial^2 u}{\partial y^2}\right) \quad (2)$$

$$\mathrm{u}\frac{\partial v}{\partial x} + v\frac{\partial v}{\partial Y} = -\frac{\partial p}{\partial y} + \frac{1}{\mathbf{Re}}\left(\frac{\partial^2 v}{\partial x^2} + \frac{\partial^2 v}{\partial y^2}\right) \quad (3)$$

The energy equation:

$$u\frac{\partial \theta}{\partial x} + v\frac{\partial \theta}{\partial y} = \frac{1}{\mathbf{RePr}}\left(\frac{\partial^2 \theta}{\partial x^2} + \frac{\partial^2 \theta}{\partial y^2}\right) \quad (4)$$

where *u*,*v*: dimensionless velocity in *x*,*y* directions, p: dimensionless pressure, Pr: Prandtl number, and θ non-dimensional temperature.

Non-dimensional Quantities

Average Nusselt number is defined as

$$\overline{Nu} = \frac{H1}{k} \cdot \frac{\bar{q}}{(\bar{T}_w - T_b)} \quad (5)$$

k: thermal conductivity of air [W/m.K] ; $\bar{q}$: avergae heat flux [W/m^2]; $\bar{T}_w$: average wall temperature of the inner wall; T_b : avergae bulk tempreture.

Local Nusselt Number at *x* location

$$\mathrm{Nu} = \frac{H1}{k} \cdot \frac{q_x}{(T_{w(x)} - T_b)} \quad (6)$$

$$T_b = (T_{in} + T_{out})/2 \quad (7)$$

Where: T_{in} is the inlet temperature [K], and T_{out} is the outlet temperature [K].

Reynolds number is defined as

$$Re = \frac{\rho u_{in} H1}{\mu} \quad (8)$$

Where ρ: density [Kg/m^3], μ: dynamic viscosity [kg/m s], u_{in}: reference velocity[m/sec].

Prandtl number can be expressed by equation (9)

$$Pr = \frac{\mu \cdot Cp}{k} \quad (9)$$

where k is thermal conductivity [W/m.K], and Cp is specific heat [J/kg.K]. To study the Prandtl number effect on forced convection heat transfer, two fluids were chosen: air where the thermal diffusivity dominates (Pr < 1), and water where momentum diffusivity dominates (Pr > 1). The physical properties of fluids are listed in Table 1[14].

Mesh independency study

To ensure the independence of the grid mesh, COMSOL multiphysics 5.5 provides different mesh density, from Extremely Coarser up to Extremely Fine. The finer mesh was chosen where the number of the elements equals 36818. The relative error in the average temperature at the exit was 0.04%.

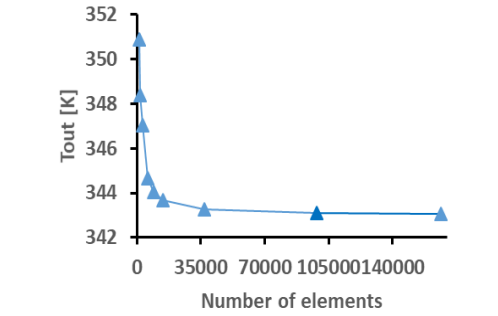

(a)

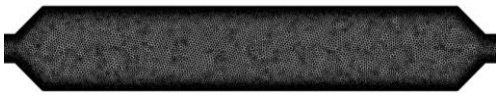

(b)

Figure 2: Mesh independency study (a) Mesh independency diagram (b) Applied mesh on the duct

With Reynolds 100 where the transmission in the flow is started from symmetry to asymmetric, the average temperature on exit with corrugated angle 45 degrees illustrated with mesh density in Figure 2(a). The meshing applied to the computational domain is illustrated in Figure 2(b).

TABLE 1: PHYSICAL PROPERTIES OF FLUIDS

Material	Thermal conductivity k, [w/m.K]	Density ρ[kg/m^3]	Prandtl number Pr	Kinematic viscosity υ[m^2/s]
Air	0.025768	1.2043	0.7077	1.5062E-5
Water	0.59423	998.2	7.1119	1.0112E-6

Validation

To validate the findings, the results were compared to the ones obtained by sparrow and chuck [15], they studied the heat transfer and fluid flow downstream from an abrupt, asymmetric channel. They consider a laminar steady forced convection and incompressibly fully developed flow. As shown in Figure 3 the agreement in the local Nusselt number is very well on the lower side of the sudden expansion channel with step height z and reattachment distance Xr.

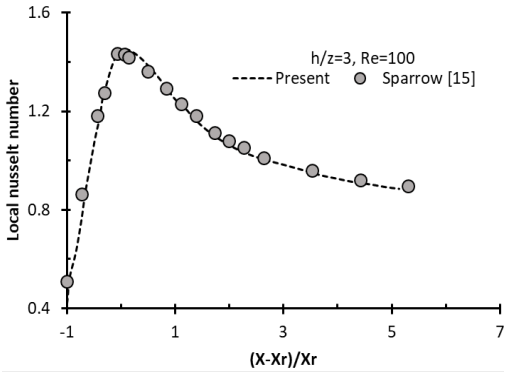

Figure 3: Local Nusselt number distribution on the lower wall.

RESULTS AND DISCUSSION

Flow separation and reattachment are essential consideration in the design of engineering equipment. For certain situations, the boundary layer greatly raises its thickness significantly in the downstream pathway by reverse flow due to flow separation, and the boundary layer flow is flipped. It contributes to the decelerated fluid particles being pushed outward, and the boundary layer is separated from the wall. Three parameters (He, α, and Re) were studied and evaluated to find the best-corrugated duct to perform better heat transfer.

Effect of Step Height

For this case, four different values of the dimensionless step height (He) are taken (0.5,1.0,1.5, and 2.0), with Reynolds number equal to 100, and the corrugation angle equal to 45 degrees. From the velocity contours in Figure 4 it can be noticed that, for He =0.5, the flow almost symmetrical, however for He>0.5, the flow becomes asymmetric. The lower wall reattachment distance and size increase slightly as the dimensionless step height increases where the size of the bubble increases, also when He>0.

The increase in step height increases the reattachment size and it is the length sharply increases on the upper wall. The effect or reattachment size can be seen in Figure 5 and 6, showing the variation of the local Nusselt number on the upper and lower walls. On the upper wall, the maximum Nusselt number decreases with increasing the step height where the bubble size increased and the cavity space occupied by low-velocity recirculating flow which is produced less convection.

On the lower wall the maximum Nusselt number increases with the step height increase, where the reattachment size is growing slightly and the bubble size smaller.

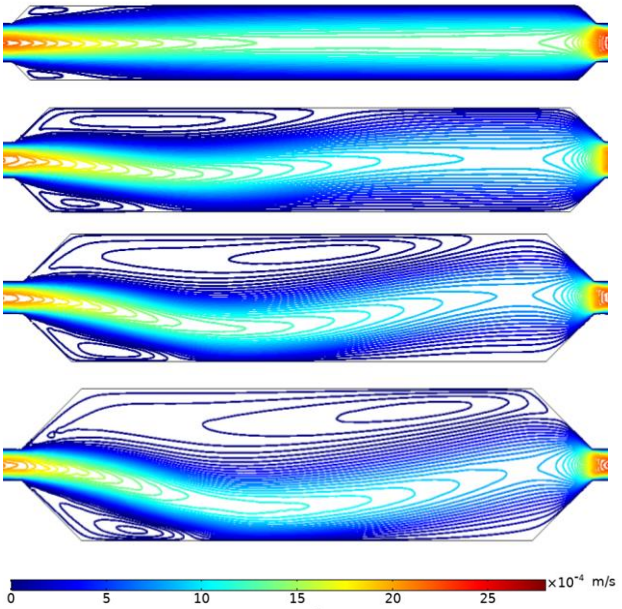

Figure 4: Velocity contour for Re=100, α=45^0, He=0.5, 1, 1.5, and 2, respectively.

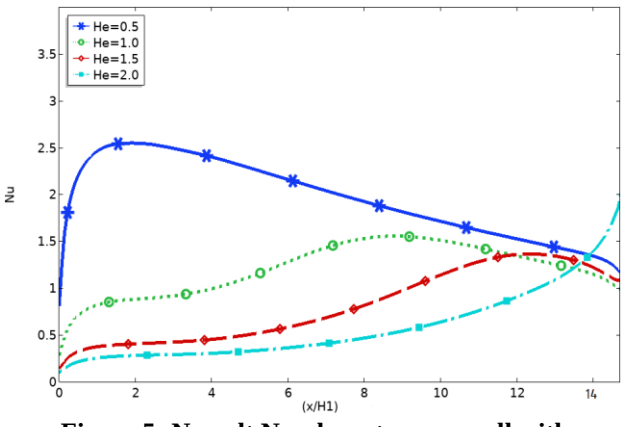

Figure 5: Nusselt Number at upper wall with Re=100, α=45^0, He=0.5,1,1.5, and2.

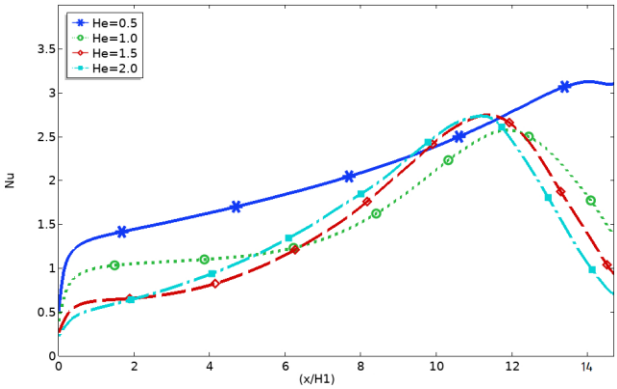

Figure 6: Nusselt Number at lower wall with Re=100, α=45^0, He=0.5,1,1.5, and 2.

To investigate the effect of step height on the distribution of temperature, Figure 7 shows the temperature contour with different step heights. When *He*=0.5 the flow distribution is symmetrical and the temperature on the lower and upper wall is equally, however as the step height increases the asymmetrical flow increases and the recirculating flow increases near the upper wall, as a result, the temperature value near the upper wall is higher than the one near the lower wall.

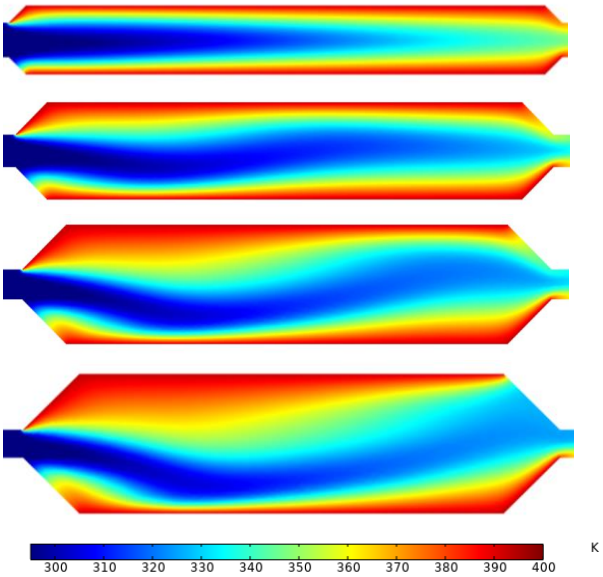

Figure 7: Temperature contours with He= (0.5, 1.0, 1.5, and 2.0, respectively), Re=100, and α=45^0

Effect of Corrugation Angle

From a Reynolds number =100 and dimensionless step height *He*=1.0 and corrugation angle has different values from 20 to 90 degrees. As the corrugation angle increases the recirculation bubble size increases dramatically near the upper wall as shown through velocity contours in Figure 8. The low-speed flow in the recirculation bubble affects the maximum value of the local Nusselt number on the upper wall, which is less than the lower wall as appearing in Figure 9. The maximum value of the local Nusselt number increases as the corrugation angle increases as illustrated in Figure 10. There is a relation between the point of reattachment and the maximum Nusselt number location, where the reattachment location corresponds to the point of maximum Nusselt number.

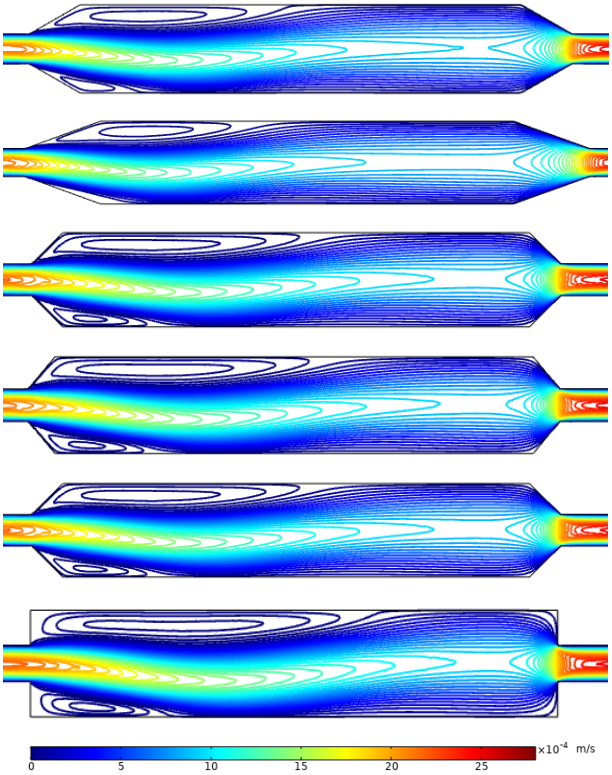

Figure 8: Velocity contours at: α=20^0, 30^0, 40^0, 45^0, 50^0, 90^0,respectively; Re=100, and *He*=1

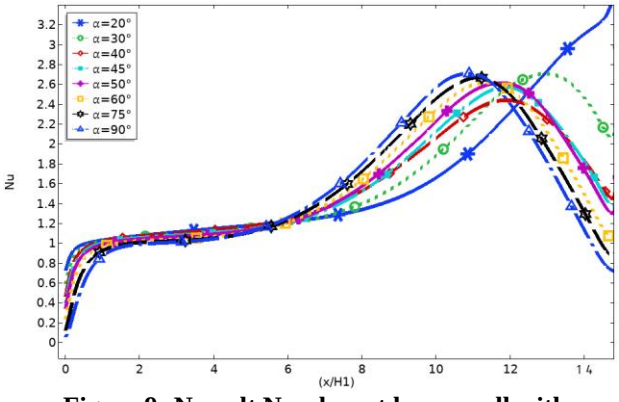

Figure 9: Nusselt Number at lower wall with different value of α, Re=100, and He=1

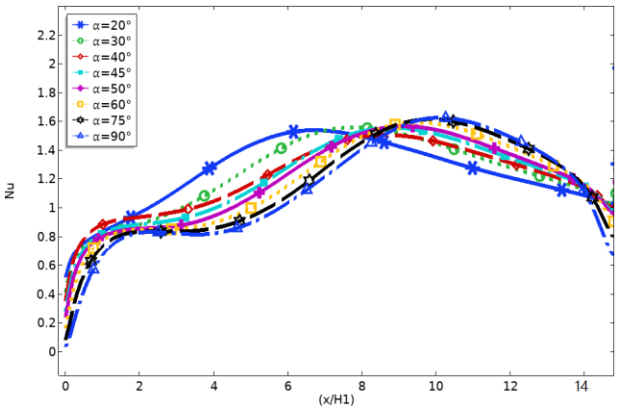

Figure 10. Nusselt Number at upper wall with different value of α, Re=100, and He=1

Effect of Reynolds Number

Five values of Reynolds number are chosen (50,100,150, 200, and 500), for α=45^0 and *He*=1.0. Figure 11 demonstrates the velocity contours with different Reynolds numbers, as Re increased the bubble size increased intensely on the upper wall while remains with constant size on the lower wall.

Figure 12 shows the variation of the upper wall Nusselt number with distance for different Re values. It shows that as the number of Reynolds increases the overall value of local Nusselt numbers at the lower wall increases, and it reaches the maximum value nearly at the same point on the lower wall for all Reynolds number values.

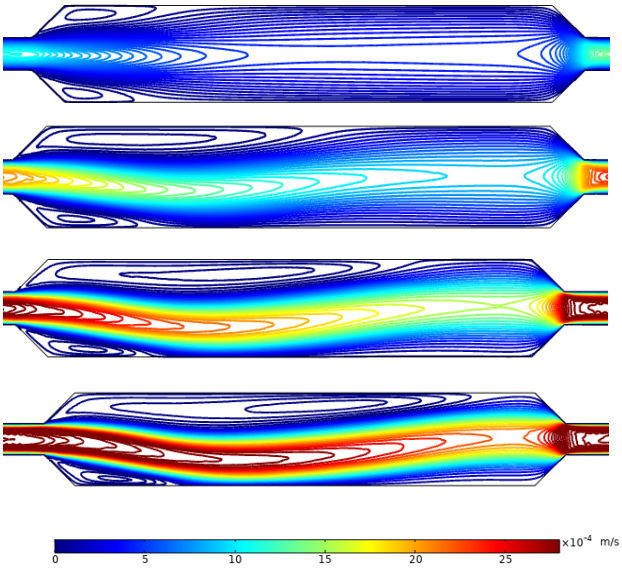

Figure 11: Velocity contours at: Re = (50, 100, 150, 200, respectively), α=45^0, and *He*=1

Figure 13 indicates the variance of the lower wall Nusselt number with distance for various Re values, the distribution of Nusselt numbers represents the separation, reattachment, and redevelopment experienced by the flow. This figure indicates that at the lower Reynolds number, the earlier achieved maximum value of the Nusselt number. The circulation bubble of the lower Reynolds number is shorter and the thermal boundary layer development downstream is higher.

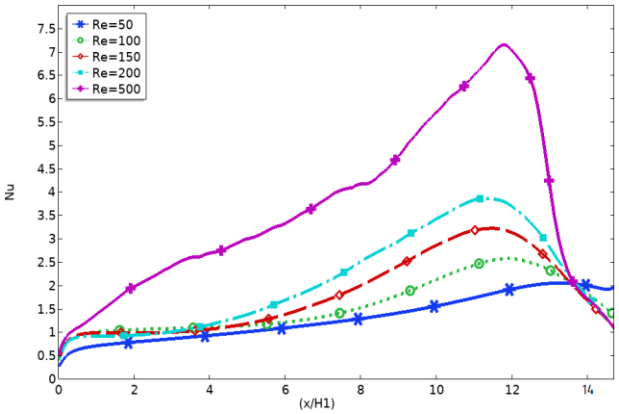

Figure 12. Nusselt number at the lower wall with Re=50-500, α=45^0, and He=1

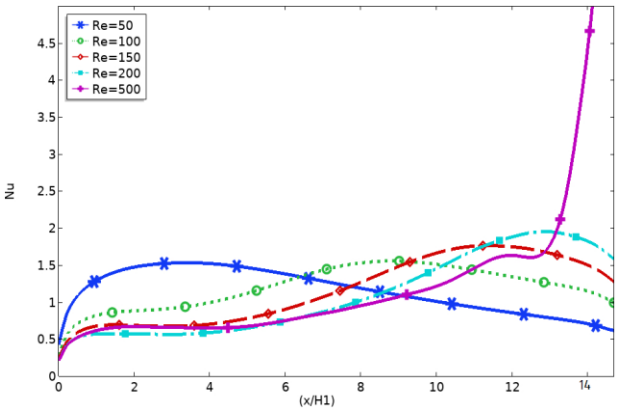

Figure 13. Nusselt number at the upper wall with Re=50-500, α =45^0, and He=1

The Efficiency of Heat Transfer

The average Nusselt number is always higher on the lower wall compare with the upper wall of the channel. The low velocity in the recirculation bubble near the upper wall reduces the convection, which affected the average Nusselt number.

Figure 14 illustrates the average Nusselt number with different step height at Re=100, α =45^0, as the step height increases the average Nusselt number decreases on both the lower and upper walls.

However, on the lower wall when He=0.5, the average Nusselt number value is above 2, and when the step height is greater than one the average Nusselt number almost remains constant.

Figure 15 shows the variation of the average Nusselt number with the corrugation angle, it displays as the corrugation angle increases the average Nusselt number decreases except when the corrugation angle is between 45 to 50 degree as a result of heat transfer enhancement near those values, it is clear that on the lower wall the value of average Nusselt number when $\alpha = 50^0$ is higher by 1% and 2% compared with $\alpha = 40^0$ and 60^0 respectively. On the upper wall, the average Nusselt number is less than the lower wall by 25%.

Figure 16 shows the average Nusselt number with different Reynolds number on the lower wall, as the Reynolds number increases the average Nusselt number increases. However, the average Nusselt number on the upper wall increases up to reach Re= 100, then it starts slightly decreases, and the effect of Reynolds number is not significant on the upper wall.

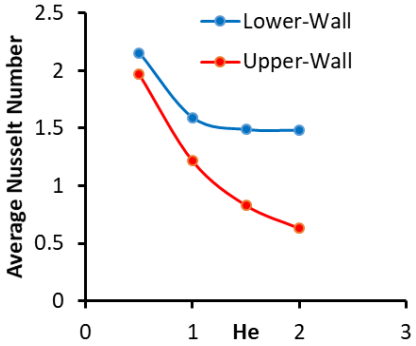

Figure 14. Average Nusselt number with different step height at Re=100, $\alpha = 45^0$

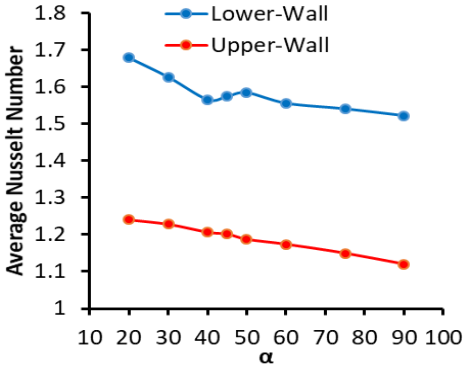

Figure 15: Average Nusselt number with Re=100, α= (20,30,40,45^0,60,75, and 90), and He=1

To study the effect of Prandtl number water was used as another fluid. The different and opposite attitude when using water was noticed on the recirculation bubble and reattachment sizes and locations. Figure17 illustrates the velocity streamlines of water with Re=100, $\alpha = 45^0$, He=1, since the bubble on the lower wall is bigger the average Nusselt number is less compared with the value on the upper wall.

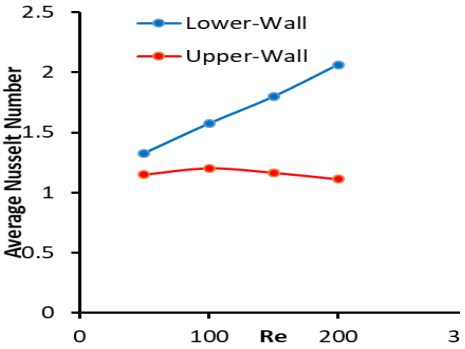

Figure 16: Average Nusselt number with different Reynolds number

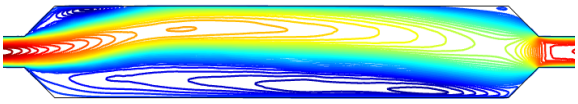

Figure 17: Velocity streamlines of water with Re=100, $\alpha = 45^0$, He=1

Figure 18 shows the Nusselt number Vs. Reynolds number with $\alpha = 45^0$, He=1 for water and air. As the P_r number rises the average Nusselt number grows, improved heat transfer at higher P_r is related to increasing into the velocity inside the bubble, increasing P_r means the decrease of thermal conductivity of fluid; as a result, the conduction decreases and the value of average Nusselt number increases.

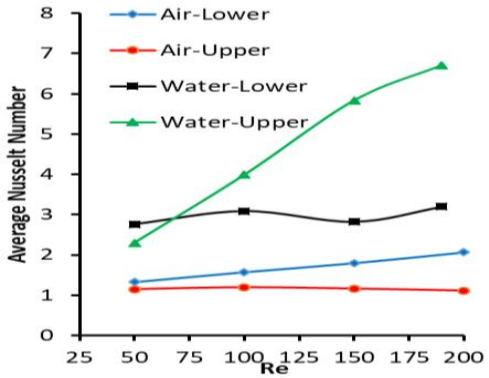

Figure 18: Water and Air average Nusselt number Vs Reynolds number with $\alpha = 45^0$, He=1.

Pressure drop

Figure 19 displays the pressure drop with different step height, and different corrugation angle. As the step height decreases the pressure drop increases, also this figure indicates that the influences of corrugation angle on the pressure drop negligible, when the corrugation angle is 45 degrees it gives the lowest pressure drop. And when *He* is 2 the pressure drop is smaller.

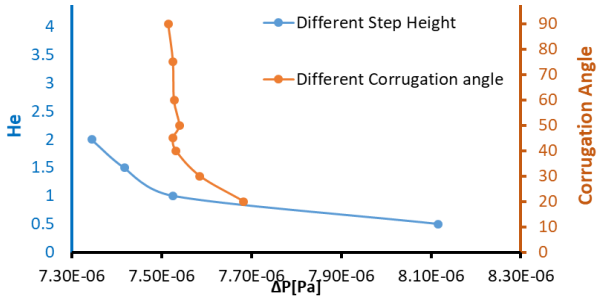

Figure 19: Pressure drop with different step heights and different corrugation angle.

CONCLUSION

In this study the hydraulic and thermal energy characteristic for laminar forced convection flow in a corrugated duct were considered. COMSOL Multiphysics 5.5 was used to solve the flow problems. From the results, we can conclude that for low Reynolds number, and a small value of dimensionless step height the flow is symmetric. The reattachment distance increases as the step height increases on the lower wall, while on the upper wall as the step height increases the recirculation bubble size increases rabidly and the maximum value of local Nusselt number decreases.

The maximum value of the local Nusselt number increases as the corrugation angle increases, when the corrugation angle between 45 to 50 degrees an enhancement of heat transfer occurred compared with other corrugation angles. A Higher Prandtl number provides better heat transfer performance. The pressure drop increases as the Reynolds number increases on the lower wall, while it is almost constant on the upper wall with the variation of Reynolds number.

REFERENCES

[1] Al zahrani S, MS Islam and SC Saha (2020). Heat transfer augmentation in retrofitted corrugated plate heat exchanger. Int J Heat Mass Transf 161: 120226.

[2] Brien JEO and EM Sparrow (2016). Corrugated-Duct Heat Transfer, Pressure Drop, and Flow Visualization. 104: 410–416.

[3] Oliveira PJ and FT Pinho (1997). Pressure drop coefficient of laminar Newtonian flow in axisymmetric sudden expansions. Int J Heat Fluid Flow 18: 518–529.

[4] Mandal DK, NK Manna, S Bandyopadhyay, BP Biswas and S Chakrabarti (2011). A numerical study on the performance of a sudden expansion with multisteps as a diffuser. Int J Appl Mech 3: 779–802.

[5] Lim JJ, HT Puay and NA Zakaria (2018). A Fundamental Study of Supercritical Flow at Sudden Expansion Structure by Using Numerical Model. 07004:

[6] Taylor C, F Group, PR Kanna, J Taler, V Anbumalar, AVS Kumar, A Pushparaj and DS Christopher (2015). Conjugate Heat Transfer From Sudden Expansion Using Nanofluid heat exchanger , cooling of turbine blade , combustion chambers , electronics cooling ,. 75–99.

[7] Fagr M (2019). Numerical study of laminar flow in a sudden expansion obstacled channel NUMERICAL STUDY OF LAMINAR FLOW.

[8] Rocha GN, RJ Poole and PJ Oliveira (2007). Bifurcation phenomena in viscoelastic flows through a symmetric 1:4 expansion. J Nonnewton Fluid Mech 141: 1–17.

[9] Zhang LZ (2005). Turbulent three-dimensional air flow and heat transfer in a cross-corrugated triangular duct. J Heat Transfer 127: 1151–1158.

[10] Metwally MN, HZ Abou-Ziyan and AM El-Leathy (1997). Performance of advanced corrugated-duct solar air collector compared with five conventional designs. Renew Energy 10: 519–537.

[11] Shockey KA, JT Pearson and DP DeWitt (1981). Heat Transfer Characteristics of a Back-Corrugated Absorber Surface for Solar Air Collectors. Am Soc Mech Eng 105:.

[12] Álvarez A, J Tarrío-Saavedra, S Zaragoza, J López-Beceiro, R Artiaga, S Naya and B Álvarez (2016). Numerical and experimental study of a corrugated thermal collector. Case Stud Therm Eng 8: 41–50.

[13] Gupta M, S Kumar and R Dudi (2011). Flow Structure and Heat Transfer Analysis in a Laminar Channel Flow with Built-in Side-by-Side Dual Triangular Prism. J Eng Technol 1: 65.

[14] Multiphysics C 3.4, COMSOL AB, Stockholm, Sweden.

[15] Sparrow EM and W Chuck (1987). PC solutions for heat transfer and fluid flow downstream of an abrupt, asymmetric enlargement in a channel. Numer Heat Transf 12: 19–40.